Spectral Polarimetric Radar Clutter Suppression to Enhance Atmospheric Echoes

CHRISTINE UNAL

Delft University of Technology, Delft, Netherlands

(Manuscript received 9 May 2008, in final form 21 February 2009)

ABSTRACT

The clutter present in the Doppler spectra of atmospheric targets can be removed by using polarimetry. The purpose is to suppress the Doppler velocity bins where spectral polarimetric parameters have atypical values. This procedure largely improves profiles of moments and polarimetric parameters of atmospheric targets. Several spectral polarimetric clutter-reduction techniques, which are based on thresholding and intended for real-time processing, are discussed in this paper. A new method, the double spectral linear depolarization ratio clutter-suppression technique, is proposed. Very satisfactory performances are obtained with this method, which can be used in the full range of elevations (0°–90°). Spectral polarimetric clutter-suppression techniques for real-time processing were studied for the S-band high-resolution Transportable Atmospheric Radar (TARA) profiler. For this study, precipitation, cloud, and clear-air scattering are considered examples of atmospheric echoes. After successful testing in 2008, the double spectral linear depolarization ratio filter was implemented in the real-time processing of the X-band scanning drizzle radar (IDRA).

1. Introduction

Removing the Doppler velocity bin 0 m s^{-1} in the Doppler spectrum of meteorological targets provides a ground clutter-suppression technique for improved measurements of reflectivity and wind. In general, this technique is not sufficient because the ground echo is not only present at 0 m s^{-1} but also in the neighboring Doppler velocity cells when high Doppler resolution ($\sim$cm s^{-1}) is required. Consequently, a notch filter, which removes a fixed number of Doppler bins around 0 m s^{-1}, is in practice implemented for weather radars. There are two drawbacks with the use of simple notch filters. First, the characteristics of the notch filter depend on the width of the ground clutter, which is variable. Second, it suppresses the narrow Doppler spectra of cloud and clear-air scattering when they are near the Doppler bin 0 m s^{-1} in the case of a profiler. Moreover, the clutter echo can be produced by moving targets, such as vehicles, airplanes, birds, and insects, which can severely contaminate the Doppler spectrum of meteorological targets.

Presently, scanning weather radars and atmospheric-profiling radars are polarimetric or will soon add polarimetric capability. Polarimetry has two major advantages. On one hand, polarimetric measurements improve the retrieval of microphysical parameters (Bringi and Chandrasekar 2001; Ryzhkov 2001). On the other hand, polarimetric clutter-suppression techniques permit to remove nonmeteorological targets (Zrnić and Ryzhkov 1999). When the probability density functions (pdfs) of polarimetric parameters between atmospheric targets and nonatmospheric targets are significantly different, a polarimetric clutter-suppression technique can be designed. When these techniques are applied on reflectivity, differential reflectivity, and wind velocity scans or profiles, data where the clutter has too severely corrupted the wanted signal are discarded, which leads to missing data. Data that are contaminated by clutter to a lesser extent will provide erroneous estimates. For example, the reflectivity may be correct, but the differential reflectivity is not.

A way to mitigate these effects is to use spectral polarimetry. It consists of combining simultaneous Doppler and polarimetric measurements of radar targets (Unal et al. 1998; Moisseev et al. 2000). Separation and characterization of different radar targets can be achieved as soon as their polarimetric responses are related to

Corresponding author address: C. M. H. Unal, International Research Centre for Telecommunication-transmission and Radar, Faculty of Electrical Engineering, Mathematics, and Computer Science, Delft University of Technology, Mekelweg 4, 2628 CD Delft, Netherlands.
E-mail: c.m.h.unal@tudelft.nl

DOI: 10.1175/2009JTECHA1170.1

different Doppler velocity bins. A spectral covariance matrix (Unal and Moisseev 2004), or covariance matrix elements for every Doppler velocity bin, can be calculated. In that case, the part of the Doppler spectrum that clearly exhibits polarimetric properties very different from the expected atmospheric targets ones is discarded. Therefore, only the relevant information for microphysical retrievals remains. In Moisseev et al. (2000), the modulus of the spectral cross-correlation coefficient is used to suppress the ground clutter spectrum in the spectrographs of precipitation (Doppler spectra of precipitation for every height or range). In Bachmann and Zrnić (2007), the use of the spectral differential reflectivity reduces the influence of bird echoes for wind retrievals. Compared to polarimetric clutter suppression, spectral polarimetric clutter-suppression techniques have the advantage of providing corrected data on the radar display instead of erroneous and missing data.

The purpose of this paper is to discuss and illustrate simple spectral polarimetric clutter-suppression techniques for real-time implementation. For this, thresholding techniques are investigated. They have to be able to work on weakly averaged or nonaveraged data. Data from the S-band Transportable Atmospheric Radar (TARA; Heijnen et al. 2000) are used for this study. Currently, averaging is part of the postprocessing and TARA typically operates at 90°, 75°, and 45° elevations. The use of X-band drizzle radar (IDRA) data collected at quasi-horizontal elevation complements this analysis.

The paper is structured as follows: section 2 briefly introduces spectral polarimetry. Sections 3, 4, and 5 give an overview of different Doppler polarimetric clutter-suppression techniques. A powerful new technique, the double spectral linear depolarization ratio filter, is introduced in section 4. The different techniques are compared on a light rain event in section 6. The performances of the double sL_{dr} filter are illustrated and discussed in section 7 for different elevations and two radar frequencies (S and X band).

2. The concept of spectral polarimetry

Spectral polarimetry is based on combined simultaneous Doppler and polarization measurements, with a close look on the polarization dependence of the radar signal per velocity bin of the Doppler spectrum. In addition to the more traditional method of expressing the Doppler spectrum in its statistical moments, spectral polarimetry can give detailed microphysical information of precipitation and clouds and separate atmospheric echoes from nonatmospheric echoes. Central to the approach are the spectrally decomposed polarization parameters. The complex Doppler velocity spectrum of the radar signal is measured for each radar resolution volume at different polarizations; for example, $S_{VV}(v)$, $S_{HV}(v)$, $S_{VH}(v)$, and $S_{HH}(v)$, with v being the Doppler velocity, and VV, HV, VH, and HH the polarization settings. From them, a spectral target covariance matrix can be calculated:

$$\mathbf{C}(v) = \begin{bmatrix} \langle S_{HH}(v)S^*_{HH}(v)\rangle & \langle \sqrt{2}S_{HH}(v)S^*_{HV}(v)\rangle & \langle S_{HH}(v)S^*_{VV}(v)\rangle \\ \langle \sqrt{2}S_{HV}(v)S^*_{HH}(v)\rangle & \langle 2S_{HV}(v)S^*_{HV}(v)\rangle & \langle \sqrt{2}S_{HV}(v)S^*_{VV}(v)\rangle \\ \langle S_{VV}(v)S^*_{HH}(v)\rangle & \langle \sqrt{2}S_{VV}(v)S^*_{HV}(v)\rangle & \langle S_{VV}(v)S^*_{VV}(v)\rangle \end{bmatrix}, \quad (1)$$

where the symbol $\langle\ \rangle$ indicates time averaging. Because of the random distribution of atmospheric particles, time averaging of the spectral target covariance matrix elements is carried out. Implicitly in (1), the reciprocity condition $S_{HV} = S_{VH}$ is applied and the matrix is polarimetrically calibrated.

The spectral reflectivity, which depends on the Doppler velocity v, is defined as

$$sZ_{XY}(v) = \langle |S_{XY}(v)|^2 \rangle. \quad (2)$$

It describes the classical Doppler power spectrum acquired with a transmitted Y polarization and a receiving X polarization, where X and Y stand for H or V. The corresponding reflectivity factor is

$$Z_{XY} = \sum_v sZ_{XY}(v). \quad (3)$$

Diverse spectral polarimetric parameters (i.e., polarimetric parameters that depend on the Doppler velocity) can be estimated from the spectral target covariance matrix (1). We shall consider three spectral polarimetric parameters for clutter suppression in this paper.

3. Clutter-suppression techniques based on the spectral cross-correlation coefficient

The first parameter discussed is the spectral cross-correlation coefficient:

$$s\rho_{co}(v) = \frac{\langle S_{VV}(v)S^*_{HH}(v)\rangle}{\sqrt{\langle |S_{HH}(v)|^2\rangle \langle |S_{VV}(v)|^2\rangle}}. \quad (4)$$

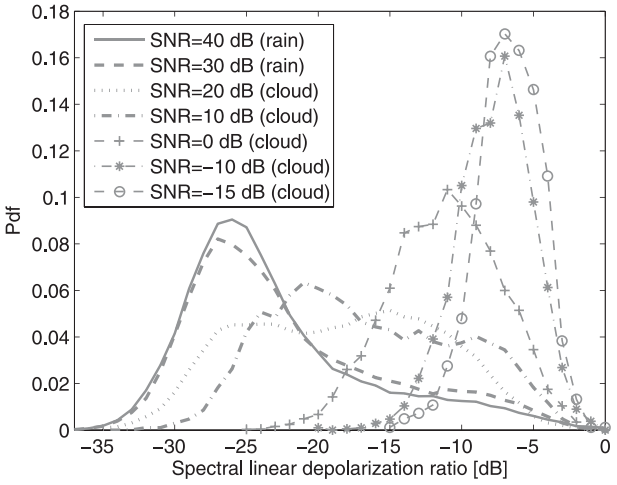

FIG. 1. Experimental pdfs of the nonaveraged spectral linear depolarization ratio values in dB for rain and precipitating cloud (19 Sep 2001). Some values of $sL_{dr}(v)$ in the left tails of the histograms are lower than TARA antenna cross-polarization isolation (−29 dB) because of statistical variations.

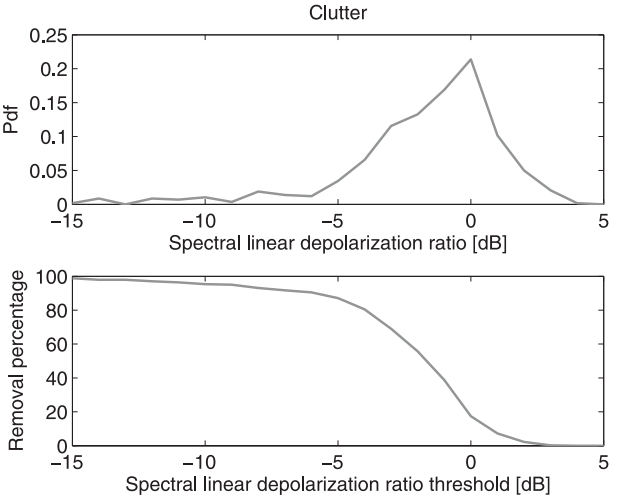

FIG. 2. (top) Experimental pdf of the spectral linear depolarization ratio for a clear-air measurement (11 Mar 2004). (bottom) The corresponding removal percentage of the clutter Doppler bins vs the selected threshold of spectral linear depolarization ratio.

In the time domain, the values of the modulus of the cross-correlation coefficient $|\rho_{co}(t)|$ are usually larger than 0.8 for weather echoes and are lower for areas contaminated by ground clutter (Ryzhkov and Zrnić 1998). This property is also applied in the Doppler domain by using the spectral cross-correlation coefficient. Earlier studies (Moisseev et al. 2000; Unal and Moisseev 2004) have shown the ability of the spectral cross-correlation coefficient to remove clutter from the atmospheric spectrographs. In Moisseev et al. (2000), the bins of the Doppler spectra related to a modulus of the spectral cross-correlation coefficient inferior to 0.8 are discarded. The limitation of this method is that it is only applicable to the sidelobe clutter (Moisseev and Chandrasekar 2009).

Subsequently, the phase of $s\rho_{co}(v)$ (i.e., the spectral differential phase) is used to develop a technique combining dealiasing and clutter suppression (Unal and Moisseev 2004). The latter technique is outlined in appendix A. Because small values of the differential phase are assumed, this procedure is currently restricted to the S band. Clutter targets with high cross-correlation between VV and HH signals can be still eliminated because of a large spectral differential phase.

4. A new clutter-suppression technique based on the spectral linear depolarization ratio

a. Introduction of the spectral linear depolarization ratio

Cross-polar measurements Z_{HV} or Z_{VH}, when available, provide powerful clutter-suppression techniques for weather radars (Hagen 1997). It is well known that the cross-polar measurements of atmospheric targets are very low compared to the copolar measurements Z_{HH} and Z_{VV}. In rain and clouds, the linear depolarization ratio L_{dr}, which is the ratio of Z_{VH} over Z_{HH}, typically exhibits values from −20 to −30 dB or lower. The lower bound of L_{dr} is governed by the cross-polarization isolation of the radar antennas (sensor limitation). The melting layer in stratiform precipitation shows the highest value, which is −15 dB, on average. A limitation for developing clutter-suppression techniques based on the linear depolarization ratio results from the fact that L_{dr} increases when the signal-to-noise ratio (SNR) decreases. For a signal-to-noise ratio close to 0 dB, the linear depolarization ratio becomes 0 dB for atmospheric targets.

One of the advantages of Doppler processing is the increase of the signal-to-noise ratio in the Doppler domain. The noise signal is decreased by a factor $1/L$, where L is the Doppler FFT length. Therefore, the use of the spectral linear depolarization ratio,

$$sL_{dr}(v) = 10\log\left[\frac{\langle S_{VH}(v)S^*_{VH}(v)\rangle}{\langle S_{HH}(v)S^*_{HH}(v)\rangle}\right] = sL^{HH}_{dr}(v), \quad (5)$$

will mitigate the aforementioned limitation.

b. Selection of the spectral linear depolarization ratio threshold

To design a spectral polarimetric filter, which has to act on nonaveraged or weakly averaged data to maintain high time resolution, the statistical variability of the

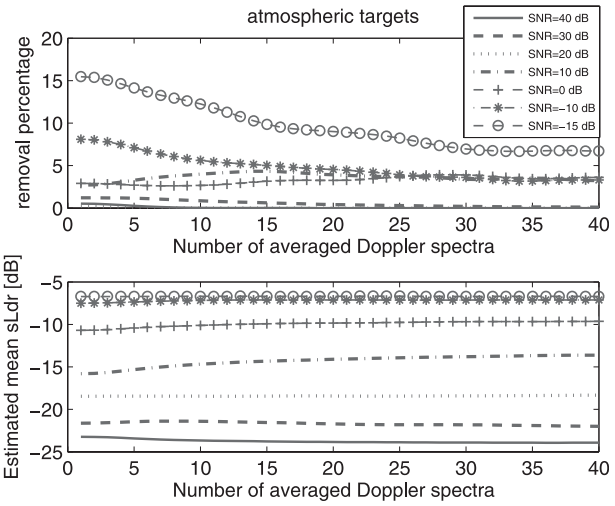

FIG. 3. (top) Removal percentage and (bottom) mean $sL_{dr}(v)$ of atmospheric targets vs the number of averaged Doppler spectra for different SNRs (19 Sep 2001). Here, 40 averages correspond to 1 min.

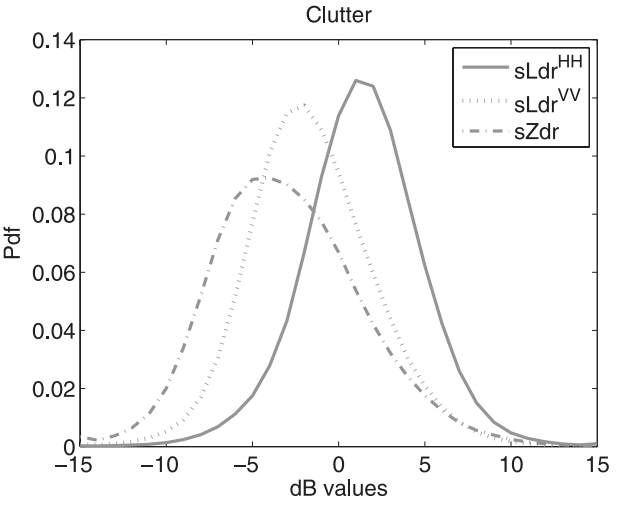

FIG. 4. Experimental pdfs of both spectral linear depolarization ratios and the spectral differential reflectivity for the clutter when TARA is pointing at 45° elevation (19 Oct 2006).

considered parameter has to be known. Hence, its probability density function or histogram has to be studied.

A representative example of histograms of spectral linear depolarization ratio in precipitation is given in Fig. 1. Here, TARA is profiling vertically. The precipitation is stratiform and moderate in intensity (19 September 2001, Cabauw, Netherlands). The measurement (acquisition of raw data) lasts 15 min. This measurement is selected because of the absence of clutter in the spectrographs (20 dB less power transmitted). Nevertheless, the Doppler bin 0 m s^{-1} is systematically removed. There is light smoothing of the Doppler spectra and a clipping of 5 dB above the Doppler noise floor is performed. After this processing, the reflectivity profiles are calculated [(3)] and all the nonaveraged Doppler bins are considered for the histograms. Figure 1 shows histograms of $sL_{dr}(v)$ in rain and precipitating cloud for different signal-to-noise ratios. The signal is the computed reflectivity factor, and the mean noise level in dBZ is known. Per height intervals, this measurement shows rather constant signal-to-noise ratios in time. These time domain signal-to-noise ratios are 40, 30, 20, 10, 0, −10, and −15 dB with standard deviations of 1.8, 1.1, 1.4, 1.3, 1.3, 3.1, and 3.4 dB, respectively. First, the mean value of $sL_{dr}(v)$ increases when the signal-to-noise ratio decreases. Second, the histograms are broad because nearly all of the Doppler spectra are used. The tails of the Doppler spectra have a Doppler signal-to-noise ratio near 5 dB because of the clipping. It would be strictly 5 dB if they were averaged.

A clear-air measurement (11 March 2004, Cabauw), with a large number of distortion lines (radar artifacts) and diverse clutter sources in the first 500 m from the radar, is made to build a histogram of spectral linear depolarization ratio (Fig. 2, top). The clutter Doppler spectra are narrow. Only the Doppler bin corresponding to the maximum spectral reflectivity is kept for the histogram. Figure 2 (bottom) shows the percentage of Doppler bins being removed versus the sL_{dr} threshold.

Based on these types of histograms, a very simple clutter-suppression technique involving a threshold on the spectral linear depolarization ratio was investigated. After considering several cases, a clipping threshold of −5 dB was chosen, which means that all the Doppler

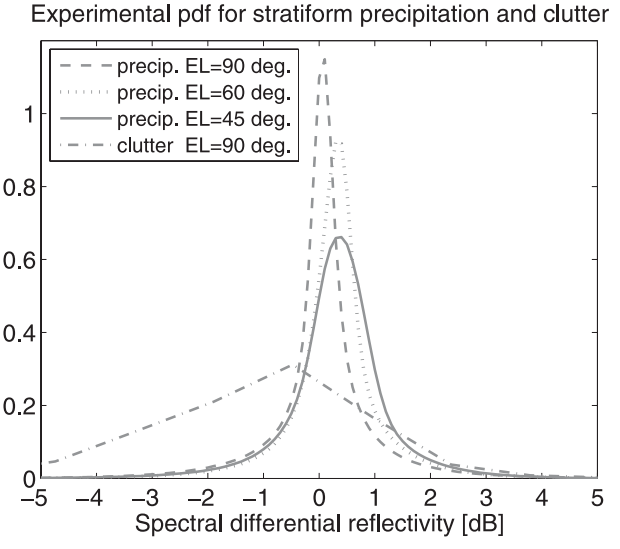

FIG. 5. Experimental pdf of $sZ_{dr}(v)$ in the case of precipitation (19 Sep 2001) and clear-air measurement (clutter; 11 Mar 2004). Precipitation consists of rain, melting layer, and precipitating cloud.

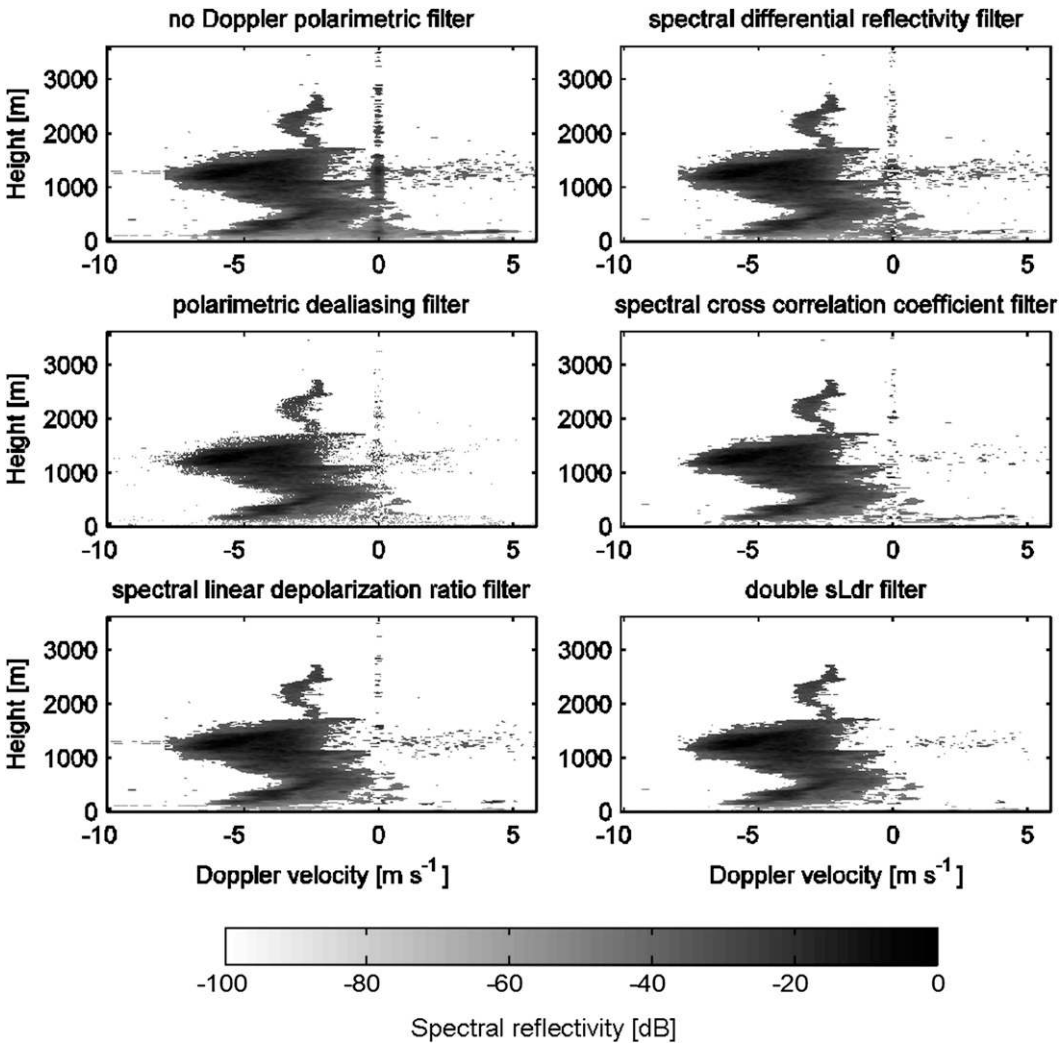

FIG. 6. Example of spectrograph of a light rain event (14 Apr 2005) processed with different Doppler polarimetric filters. A spectrograph consists of Doppler spectra for every height or range. The elevation is 75°.

bins of the spectral covariance matrix that correspond to $sL_{dr}(v) > -5$ dB are discarded. For the clear-air measurement, the removal percentage of the clutter for a sL_{dr} clipping of -5 dB is 87%.

c. Melting layer

To obtain Fig. 1, the melting-layer data were avoided. The Doppler spectra of the melting layer have extended tails, with still-sufficient Doppler signal-to-noise ratio, but atypical spectral polarimetric properties (high sL_{dr} larger than -5 dB and low spectral cross-correlation coefficient below 0.7). Consequently, these tails are suppressed with spectral polarimetric filtering. For profiling only, the main peak contributes to the computation of the moments. For a thorough study of the melting-layer spectral covariance matrix, this sL_{dr} filter and the spectral cross-correlation coefficient filter (modulus or phase) should not be applied.

d. Averaging

Looking again at Fig. 1, low reflectivity clouds may be partially suppressed by this spectral polarimetric clutter-suppression technique. This cloud suppression increases when the signal-to-noise ratio decreases. Figures 1 and 2 are based on nonaveraged spectrographs. The averaging depends on the type of atmospheric target and on the selected atmospheric parameter or application. Figure 3 illustrates the removal percentage of atmospheric targets (top) and the mean $sL_{dr}(v)$ (bottom) versus the number of Doppler spectra averaged for different signal-to-noise ratios.

With the average, on one hand, we expect less statistical variations and then a narrowing of the distributions.

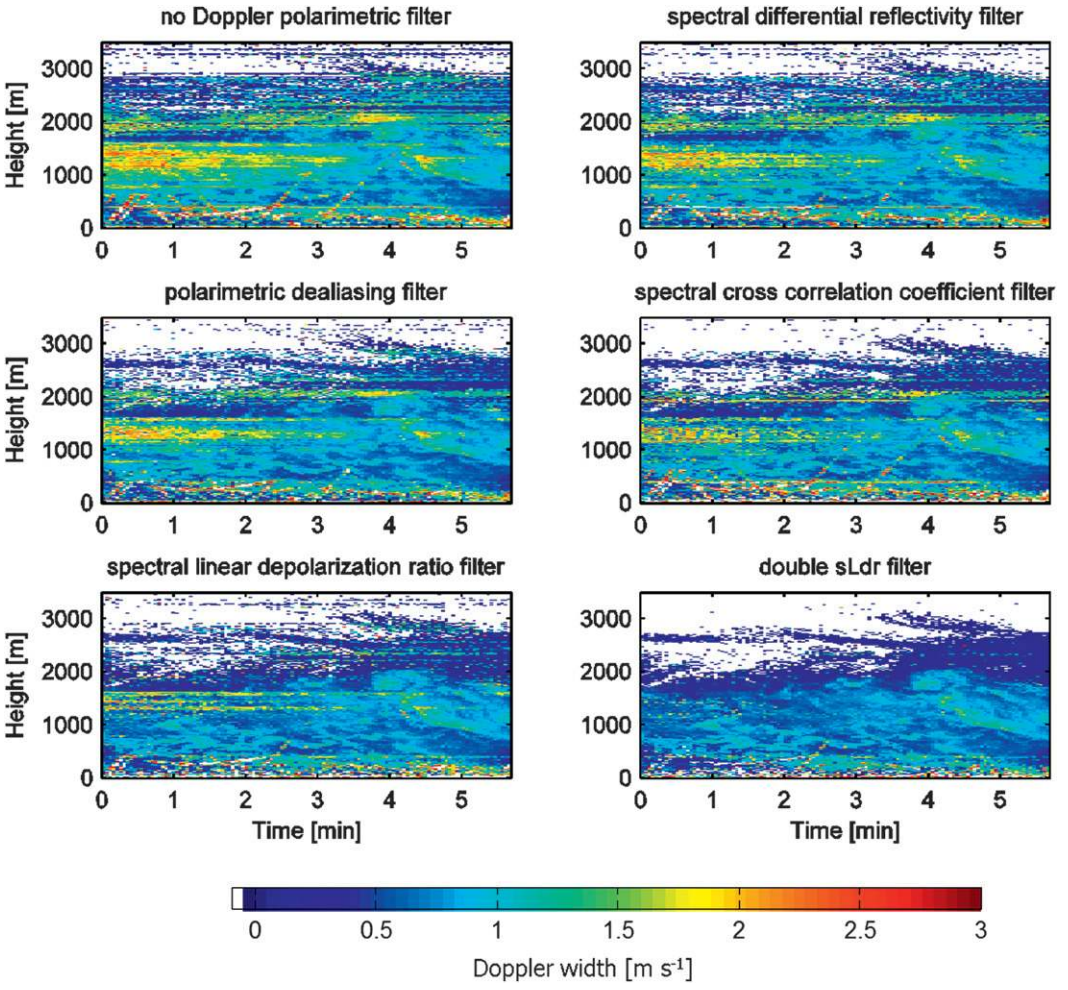

FIG. 7. Doppler width profiles (14 Apr 2005) obtained after applying different Doppler polarimetric filters. Note the oblique lines of erroneous data resulting of weak echoes of moving vehicles. The best Doppler polarimetric filter is the new double spectral linear depolarization ratio filter. The comparison of the two lowest plots shows the enhancement of the filter by applying a clip for both spectral linear depolarization ratio parameters instead of one.

On the other hand, the Doppler signal-to-noise ratio is variable from large at the top of the Doppler spectrum to 5 dB (minimum) at the tails of the Doppler spectrum, which limits the narrowing of the distributions. Consequently, from a limited narrowing of the distribution, we expect a decrease of the removal percentage of atmospheric targets with averaging. This is generally the case in Fig. 3 (top). The estimated mean $sL_{dr}(v)$ stays rather constant with averaging and is strongly dependent on the signal-to-noise ratio (Fig. 3, bottom). Two curves are deviating from the expected trends (SNR = 10 dB and SNR = 0 dB). They show an increase both in removal percentage of hydrometeors and in mean $sL_{dr}(v)$ when the averaging increases. The corresponding Doppler spectra exhibit a significant variation of the vertical wind with time, which prohibits a ''blind'' averaging. For the case SNR = −15 dB with no average, there are too many missing data in the Doppler spectrum and averaging is necessary to obtain a Doppler spectrum.

The removal percentage should decrease when the signal-to-noise ratio increases. Compared to SNR = 30 dB and SNR = 40 dB, the curve SNR = 20 dB deviates slightly, giving better results in removal percentage. This can happen when the tails of experimental histograms built from a finite number of data are considered.

Summarizing, for high SNR (40, 30, and 20 dB), the removal percentage of atmospheric targets is less than 2%. For low SNR (10 and 0 dB), it is less than 5%. It is less than 10% for negative SNR (−10 and −15 dB), the latter after averaging 15 Doppler spectra (23 s). For spectral polarimetric parameters, averaging is a critical issue and an appropriate averaging procedure on the spectrographs should be investigated.

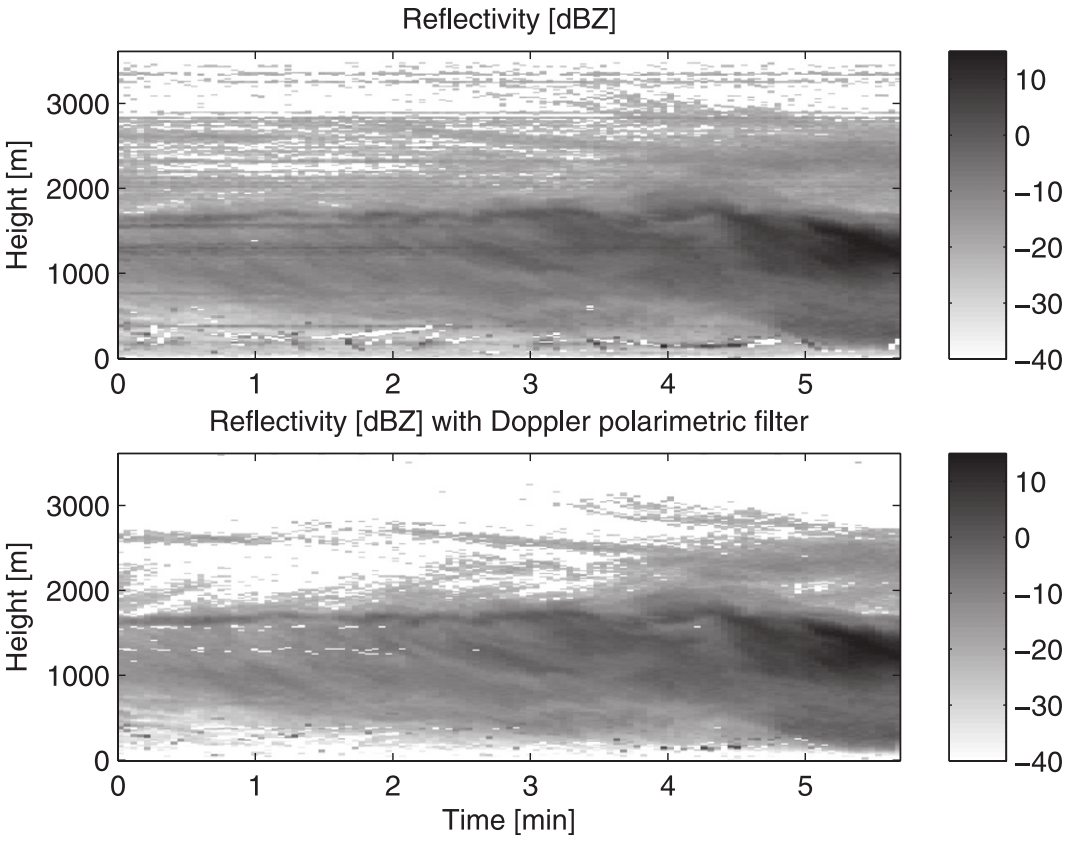

FIG. 8. Reflectivity profiles of light rain (14 Apr 2005) contaminated by clutter. The time resolution is 3 s and the height resolution is 14.5 m.

e. First concluding remarks

The spectral linear depolarization ratio filter with a threshold of −5 dB substantially removes the clutter (e.g., 87% in Fig. 2) and will enhance rain and cloud echoes with sufficient Doppler signal-to-noise ratio. Though largely biased by noise (Fig. 3, bottom), this parameter, which most of the time cannot be used for the microphysics of rain and clouds, provides a very good clutter-suppression technique. Compared to the polarimetric dealiasing clutter-suppression technique with a clutter reduction of 66%, the $sL_{\rm dr}$ filter has a better performance.

f. Enhancement of the spectral linear depolarization ratio filter: Double sL_{dr} filter

By calculating the ratio of the Doppler power spectrum HV over the Doppler power spectrum VV, the spectral linear depolarization ratio

$$sL_{\rm dr}^{\rm VV}(v) = 10\,\log\left[\frac{\langle S_{\rm HV}(v)S_{\rm HV}^{*}(v)\rangle}{\langle S_{\rm VV}(v)S_{\rm VV}^{*}(v)\rangle}\right] \qquad (6)$$

is obtained. The enhancement of the spectral linear depolarization ratio filter consists of applying the spectral linear depolarization ratio filter, using both $sL_{\rm dr}^{\rm HH}(v)$ [(5)] and $sL_{\rm dr}^{\rm VV}(v)$ [(6)] with the same threshold of −5 dB.

The important advantage of the double $sL_{\rm dr}$ filter is that it suppresses more clutter than a single $sL_{\rm dr}$ filter without significantly further removing atmospheric target echoes. For reciprocal scattering ($S_{\rm VH} = S_{\rm HV}$), their difference is

$$sL_{\rm dr}^{\rm VV}(v) - sL_{\rm dr}^{\rm HH}(v) = sZ_{\rm dr}(v) = 10\,\log\left[\frac{\langle S_{\rm HH}(v)S_{\rm HH}^{*}(v)\rangle}{\langle S_{\rm VV}(v)S_{\rm VV}^{*}(v)\rangle}\right], \qquad (7)$$

where $sZ_{\rm dr}(v)$ is the spectral differential reflectivity. For vertical profiling, $sL_{\rm dr}^{\rm HH}(v)$ and $sL_{\rm dr}^{\rm VV}(v)$ have the same range of values for hydrometeors. This implies no further reduction of the atmospheric echoes when both spectral parameters are used for clutter filtering. This is different for the clutter, which has different properties when measured with horizontal and vertical polarization. Extra clutter reduction then occurs.

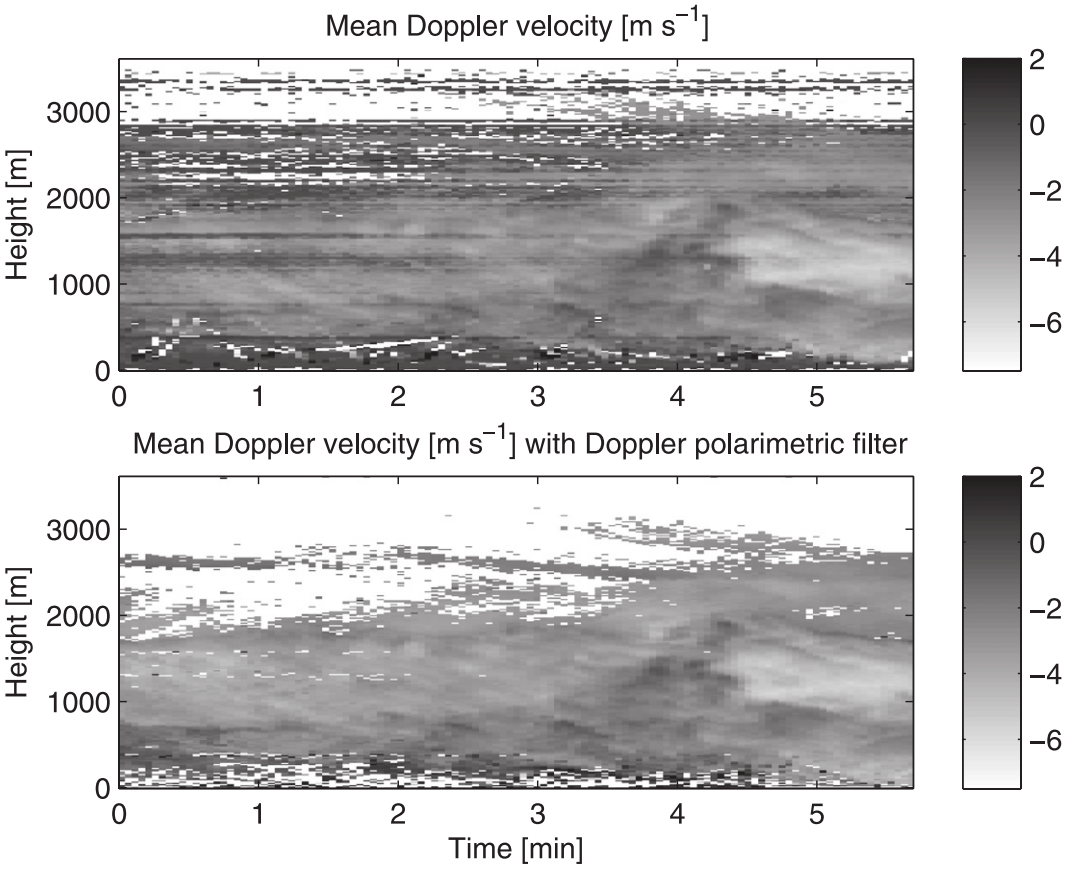

FIG. 9. Mean Doppler velocity profiles. The negative Doppler velocities indicate that the targets approach the radar. The elevation is 75°, which means that the fall velocity of the hydrometeors and the local wind contribute to the mean Doppler velocity.

Figure 4 presents the clutter properties in the boundary layer (19 October 2006, Cabauw) at the elevation of 45°. In this case, the spectral differential reflectivity has a negative trend, which implies that a majority of the $sL_{dr}^{VV}(v)$ values are smaller than the $sL_{dr}^{HH}(v)$ values. For this example, the clipping on $sL_{dr}^{HH}(v)$ removes most of the clutter.

The spectral linear depolarization ratios depend on the type of hydrometeors, the radar elevation, and the frequency. However, both parameters have small values for atmospheric targets and the threshold of −5 dB is rather high. At quasi-horizontal elevations, when the rain rate increases, $sL_{dr}^{VV}(v)$ becomes larger than $sL_{dr}^{HH}(v)$. However, because of the increase in signal-to-noise ratio, there is no further reduction of rain echoes. Therefore, it is expected to have good results with this technique from 90° to 0° elevations. Illustration is given in section 7 for the 75°, 45°, and 0.5° elevations. Huge improvements after applying the double sL_{dr} filter have been observed.

The techniques, single sL_{dr} filter and double sL_{dr} filter, are also considered for higher frequencies than the S band. An example will be given in section 7 for the X band. In case of propagation effects, $sL_{dr}^{HH}(v)$ is increased by differential attenuation, whereas $sL_{dr}^{VV}(v)$ is decreased by the same differential attenuation. Therefore, the sum $sL_{dr}^{VV}(v) + sL_{dr}^{HH}(v)$ could be used for spectral polarimetric filtering. Research work has to be done for this purpose to be conclusive.

5. Clutter-suppression technique based on the spectral differential reflectivity

The spectral differential reflectivity (7) represents the Doppler spectrum of Z_{dr}, where Z_{dr} is the ratio of Z_{HH} over Z_{VV}. The function $sZ_{dr}(v)$ depends on the particle size distributions of atmospheric hydrometeors present in the radar resolution volume, on the mean Doppler wind velocity, and on the turbulence spectrum. New retrieval techniques, which are using the measurement of this spectral polarimetric parameter in the case of slant profiling, have been recently proposed. The possibility to retrieve two particle size distributions (plates and aggregates) from monomodal Doppler spectra above the

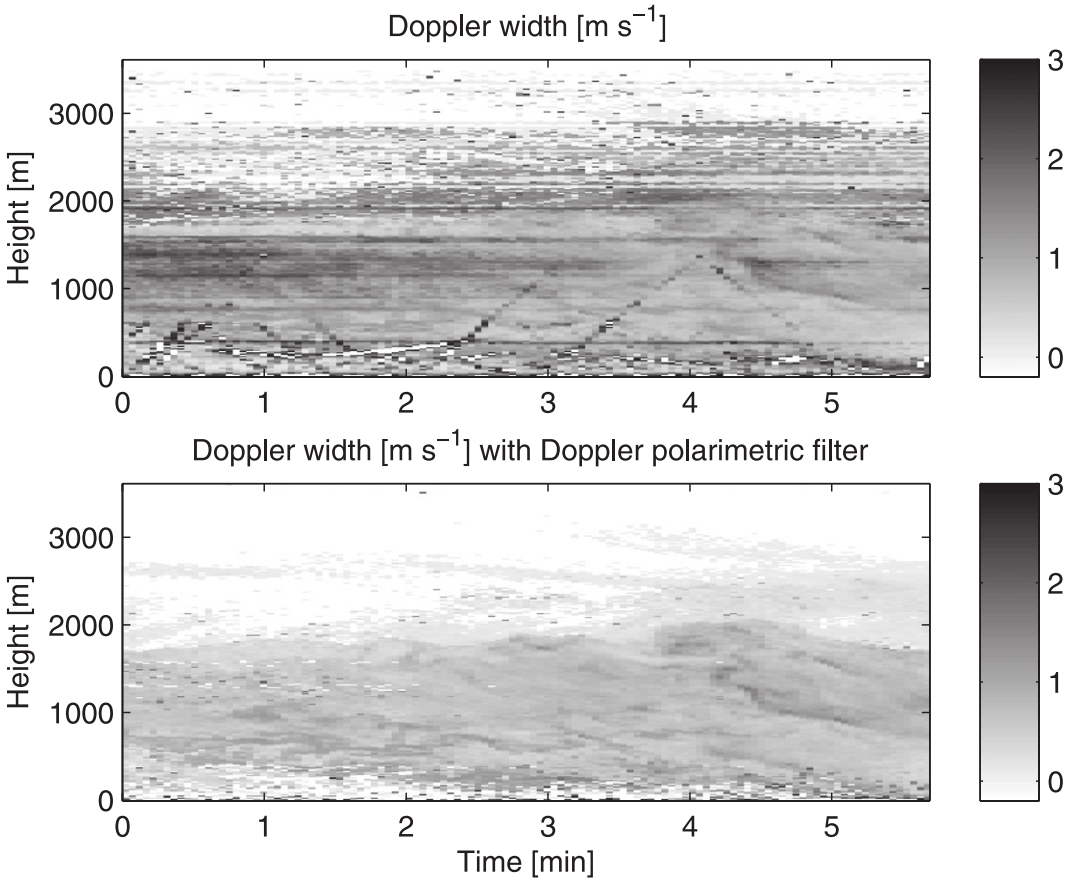

FIG. 10. Doppler width profiles. Note the increase in Doppler width when there is a sudden increase of reflectivity (4–5 min).

melting layer is investigated in Spek et al. (2008). The raindrop size distribution is obtained without assumption on its shape after deconvolution of the Doppler spectrum in Moisseev and Chandrasekar (2007). A method to estimate the eddy dissipation rate in rain, based on $sZ_{dr}(v)$, is proposed in Yanovsky et al. (2005). The spectral differential reflectivity is also investigated for clutter suppression in Bachmann and Zrnić (2007) to separate bird and insect echoes for wind retrievals.

The experimental probability density function of $sZ_{dr}(v)$ for precipitation is given at different elevation angles in Fig. 5. Three datasets of 15 min each acquired 19 September 2001 at the 90°, 60° and 45° elevations are used. To build these probability density functions, the tails of the Doppler spectrum of the melting layer are not considered. The distributions show that a threshold of 5 dB may be implemented for the real-time measurements of TARA at the elevations of 45°–90°. The Doppler bins related to a modulus of the spectral differential reflectivity larger than 5 dB are discarded. For weather radars scanning at quasi-horizontal elevations, Z_{dr} values can be larger than 5 dB (Meischner et al. 1991) and then the threshold of 5 dB for $|sZ_{dr}(v)|$ is too low. Considering the distributions of $sZ_{dr}(v)$ for both clear-air measurements at 90° (Fig. 5) and 45° (Fig. 4) elevations, the effectiveness of this clutter suppression will be limited.

6. Comparison of the spectral polarimetric clutter-suppression techniques

A light rain event (14 April 2005, Cabauw), which is severely contaminated by distortion lines, ground clutter, and moving clutter, is chosen to compare the following spectral polarimetric clutter-suppression techniques:

- no Doppler polarimetric filter;
- spectral differential reflectivity filter (section 5);
- polarimetric dealiasing filter (appendix A);
- spectral cross-correlation coefficient filter (modulus; section 3);
- spectral linear depolarization ratio filter (section 4b); and
- double sL_{dr} filter (section 4f).

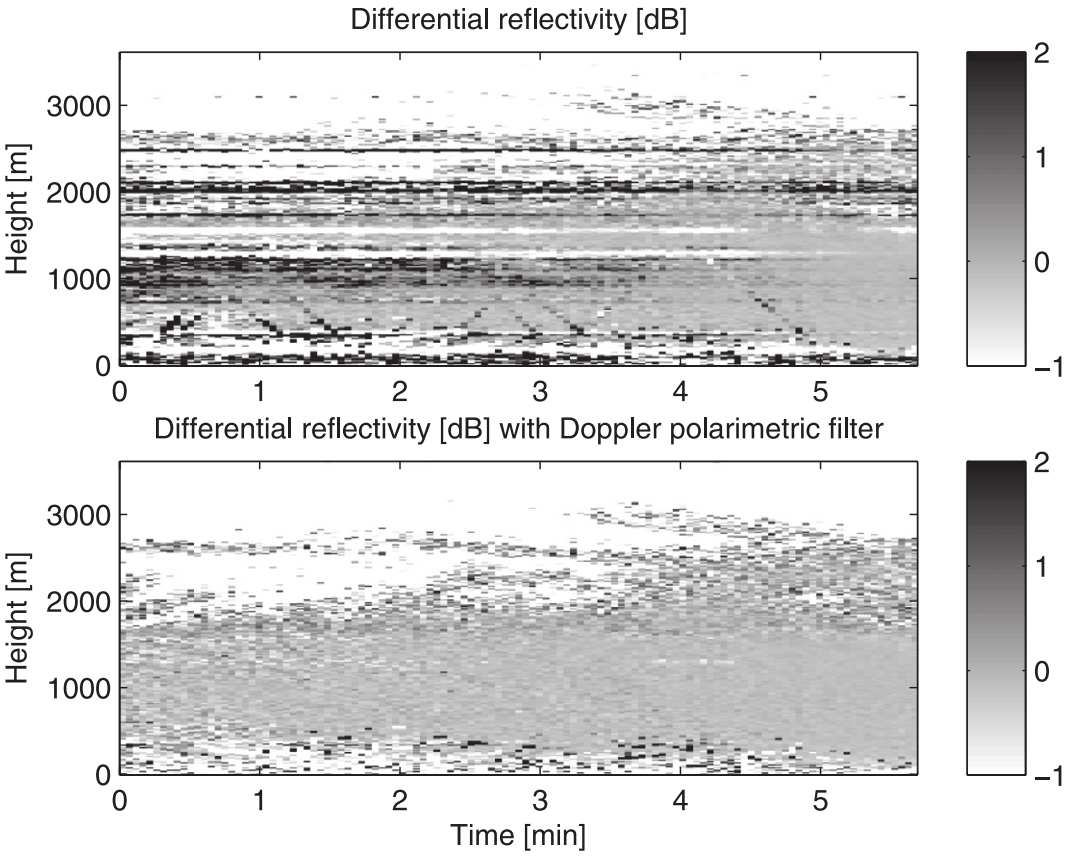

FIG. 11. Differential reflectivity profiles.

The processing is described in appendix B.

a. Comparison of ground clutter

Examples of spectrographs are given in Fig. 6. They represent the spectral reflectivity (2). The large Doppler spectra (0–1600 m) are related to rain and the narrow ones to the precipitating cloud. The Doppler velocity is negative when the targets approach the radar. High Doppler resolution spectral polarimetric measurements are necessary for cloud microphysical retrievals (Spek et al. 2008). In that case, the ground clutter Doppler spectrum may consist of 13 Doppler bins with a Doppler resolution of 3 cm s^{-1}. This ground clutter band around 0 m s^{-1}, from -0.2 to 0.2 m s^{-1}, is well visible in Fig. 6 and is the best removed by the double spectral linear depolarization ratio filter. The useful part of the spectrograph is well preserved by all the spectral polarimetric filters. There are missing data in the spectrograph after the polarimetric dealiasing clutter suppression technique based on the phase of $s\rho_{co}(v)$. Interpolation may be necessary in this case. Applying only the spectral differential reflectivity filter does not provide a satisfactory clutter reduction.

b. Comparison of moving clutter

Because spectral polarimetric clutter-suppression techniques are compared, profiles of a nonpolarimetric parameter, the Doppler width, are selected (Fig. 7). This parameter is highly sensitive to clutter.

The first artifact, well visible in Fig. 7 (top), consists of horizontal lines in the time–height representation. They are caused by the radar itself (distortion lines). This problem, which depends on the measurement specifications, occurs at random Doppler velocities. This is an example of a bad case with multiple distortion lines. Figure 7 (bottom right) shows that the double $sL_{dr}(v)$ clipping eliminates this artifact.

Another source of clutter consists of weak echoes of moving vehicles on a nearby small road picked up by the sidelobes of the antenna patterns. They pollute the profiles in the boundary layer until 1500 m, and they draw oblique lines of erroneous data in the time–height representation. Only the filters based on the spectral linear depolarization ratios (Fig. 7, bottom) and on the spectral differential phase (Fig. 7, middle left) can substantially reduce them.

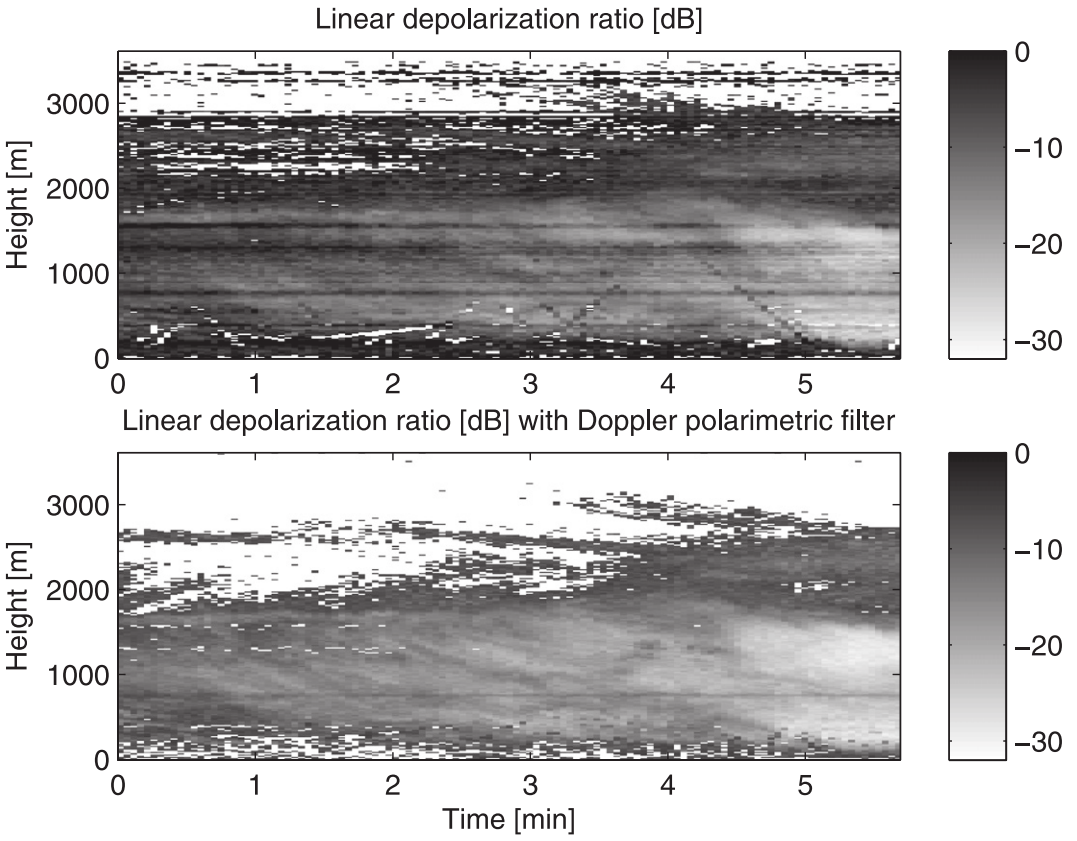

FIG. 12. Linear depolarization ratio profiles. After filtering, the large values of L_{dr} above 1600 m are caused by a low SNR.

For these types of moving clutter targets (including distortion lines), the double spectral linear depolarization ratio clipping of −5 dB provides the best suppression. The other techniques, $sZ_{dr}(v)$ filter, polarimetric dealiasing clutter suppression, $|s\rho_{co}(v)|$ filter, and $sL_{dr}(v)$ filter, reduce clutter but are not as effective as the double $sL_{dr}(v)$ filter.

c. *Suggested use of algorithms based on spectral polarimetry*

For a full polarimetric radar that measures S_{HH}, S_{VV}, and S_{HV}, the double spectral linear depolarization ratio clutter suppression technique is recommended. Because clutter with small $sZ_{dr}(v)$ values can also be eliminated with the double $sL_{dr}(v)$ filter, this method performs better than a combination of the $sZ_{dr}(v)$ filter with the single $sL_{dr}(v)$ filter. When the radar only transmits one polarization (H or V) and receives with a dual-polarized receiver (H and V), then the single spectral linear depolarization ratio filter should be used.

When the cross-polar measurement is not available, such as in the case of the simultaneous transmission and reception (STAR) mode, at quasi-horizontal elevation, thresholding on the spectral cross-correlation coefficient can be investigated. A threshold of 0.8 for the modulus of $s\rho_{co}(v)$ will reduce sidelobe clutter. At the S band, the phase of $s\rho_{co}(v)$ or spectral differential phase can be clipped when it exceeds the interval $[-s\psi_{max}, s\psi_{max}]$ to partially remove side- and main-lobe clutter. To choose $s\psi_{max}$ the ranges of propagation path and rain rate should be considered (Unal and Moisseev 2004). For the STAR mode, this technique, based on the complex spectral cross-correlation coefficient thresholding, which can be easily implemented in real time, can be compared with a very recently proposed technique (Moisseev and Chandrasekar 2009) based on a fuzzy logic algorithm that is applied to the modulus of the spectral cross-correlation coefficient and to the textures of spectral differential phase and spectral differential reflectivity.

7. Spectral polarimetric processing: Illustration and discussion

The spectral polarimetric processing (appendix B), which is currently applied to TARA study cases and recent campaigns (2007–08), is discussed in terms of

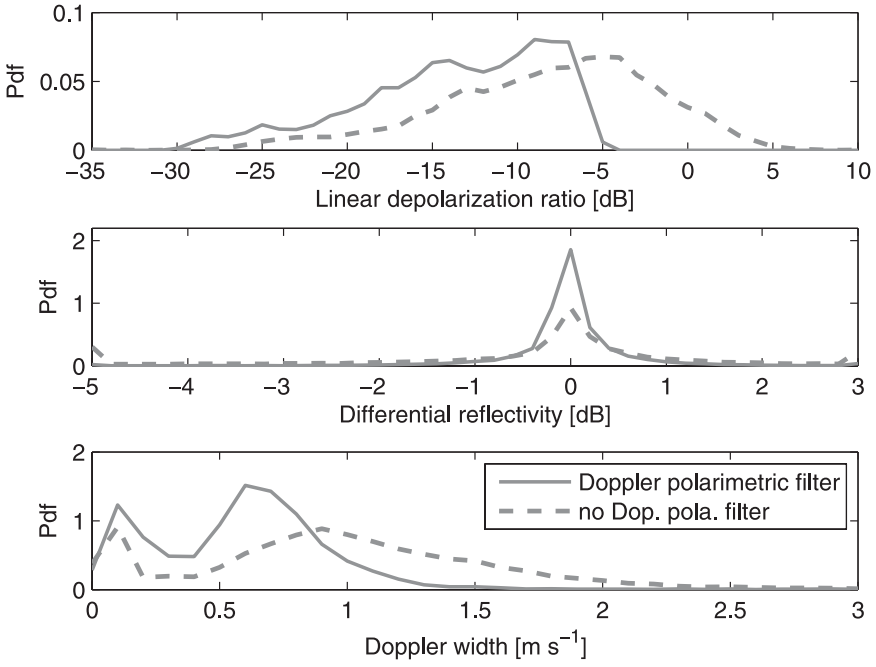

FIG. 13. Experimental pdfs based on the profiles of light rain (14 Apr 2005). The distributions show a more realistic behavior for light precipitation after Doppler polarimetric clutter suppression.

clutter suppression. The main contributor to clutter reduction is the double $sL_{dr}(v)$ filter. Its performances are illustrated and discussed for the 75° and 45° elevations at the S band. Furthermore, the technique is illustrated for the 0.5° elevation at the X band.

a. Near-vertical profiling with the 75° elevation

The light rain event (14 April 2005, Cabauw) measured by TARA is plotted as profiles in Figs. 8–12. The top panels of Figs. 8–12 show the moments (reflectivity Z_{HH}, mean Doppler velocity v_{HH}, and Doppler width W_{HH}), the differential reflectivity Z_{dr}, and the linear depolarization ratio L_{dr} versus time and height without spectral polarimetric clutter suppression, respectively. The bottom panels of Figs. 8–12 present the same parameters after the currently optimum spectral polarimetric processing, which consists of the double $sL_{dr}(v)$ filter combined with the polarimetric dealiasing clutter-suppression technique.

The distortion lines and the oblique lines resulting from vehicles on a nearby road are effectively eliminated in the bottom panels of Figs. 8–12. The erroneous data are replaced by data that are consistent with the neighboring parameter values. There is also a moving tractor in a field. The most visible consequence of this echo is a piece of a white parabolic line in the first 500 m around 2 min (top panel). This echo is well suppressed in the bottom panels of Figs. 8–12. The main clutter suppression results from the double spectral linear depolarization ratio filter. Because of the need of a robust dealiasing technique for slant profiling, polarimetric dealiasing is applied. Adding its clutter-reduction action improves the profiling. Both techniques suppress moving clutter but not always the same (see Fig. 6), causing their combination to be quite efficient.

Consequently, the parameters, Z_{HH}, v_{HH}, W_{HH}, Z_{dr}, and L_{dr} are considerably improved. The mean Doppler velocity profiles (Fig. 9, bottom) and the Z_{dr} profiles (Fig. 11, bottom) now show continuous meaningful patterns. The Doppler width becomes smaller in former clutter-contaminated areas. As the result of the spectral polarimetric clutter suppression, fine details, such as the broadening of the Doppler spectrum because of changes in the drop size distribution or turbulence, can now be seen on the Doppler width profiles (Figs. 7, 10, bottom). After filtering, weak cloud echoes can have their reflectivity and Doppler width underestimated, but their polarimetric properties and mean Doppler velocity are generally improved.

Comparing the top and bottom panels of Figs. 8–12, 20% of the data are clutter and are removed with spectral polarimetry. Suppose that all the time–height bins related to $L_{dr} > -5$ dB are discarded; with this polarimetric filter, 34% of the data would be suppressed. Moreover, after polarimetric filtering, 13% of the

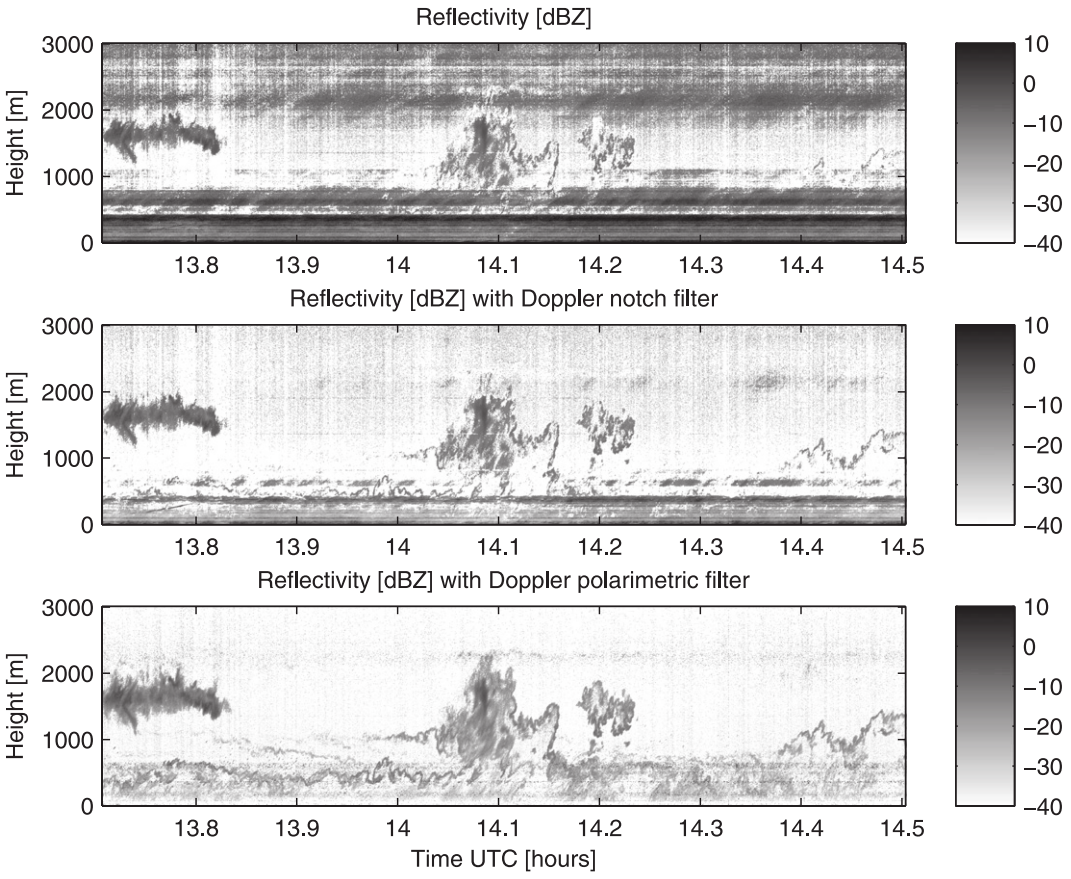

FIG. 14. Profiles of cloud and clear-air scattering in the boundary layer (9 Jul 2007; height resolution 5.9 m). During the COPS campaign, the measurements at 45° elevation are strongly contaminated until 900 m by a clutter band; this band is suppressed by the Doppler polarimetric filter, which reveals here the weak echoes of clear-air scattering.

remaining data have $|Z_{dr}|$ values larger than 1, which is not expected, compared to 7% after spectral polarimetry.

Resulting histograms are plotted in Fig. 13. After Doppler polarimetric clutter suppression, the distributions of L_{dr}, Z_{dr}, and W_{HH} are more realistic for light precipitation. The distribution of L_{dr} now points out a larger amount of negative values from −30 to −7 dB. The distribution of Z_{dr} is narrowed around 0 dB, which is expected at near-vertical elevation. Note the absence of tails in the pdf of the filtered Z_{dr}. The distribution of the Doppler width is narrower with values from 0.03 to 1.5 m s^{-1}. Large values from 1.5 to 2.5 m s^{-1} are not present anymore. The Doppler widths from 0.03 to 0.05 m s^{-1} leading to the 0 m s^{-1} bin are obtained for cloud Doppler spectra near the Doppler noise level. In the profiles and the resulting probability density functions, the clutter-contaminated data are not only suppressed, but a large amount of them are corrected.

b. *Slant profiling at 45° elevation*

The complete set of spectral polarimetric clutter-suppression techniques is developed and successfully tested on measurements carried out at Cabauw (flat field area). The double $sL_{dr}(v)$ filter combined with the polarimetric dealiasing clutter-suppression technique is next applied on the measurements of the Convective Orographically-induced Precipitation Study (COPS) campaign in the Black Forest of Germany during the summer of 2007. There, TARA is located at the top of a mountain, where various sources of clutter can be measured through the sidelobes of the antenna patterns (mountains, trees, towers, and other sensors that are placed at 250-m distance). When the elevation decreases from 90° (vertical profiling) to 45°, the clutter contamination of the atmospheric data increases. Figure 14 displays processed profiles (9 July 2007) obtained with the 45° elevation, without filter (top panel), with a classical notch filter (middle panel), and with the Doppler

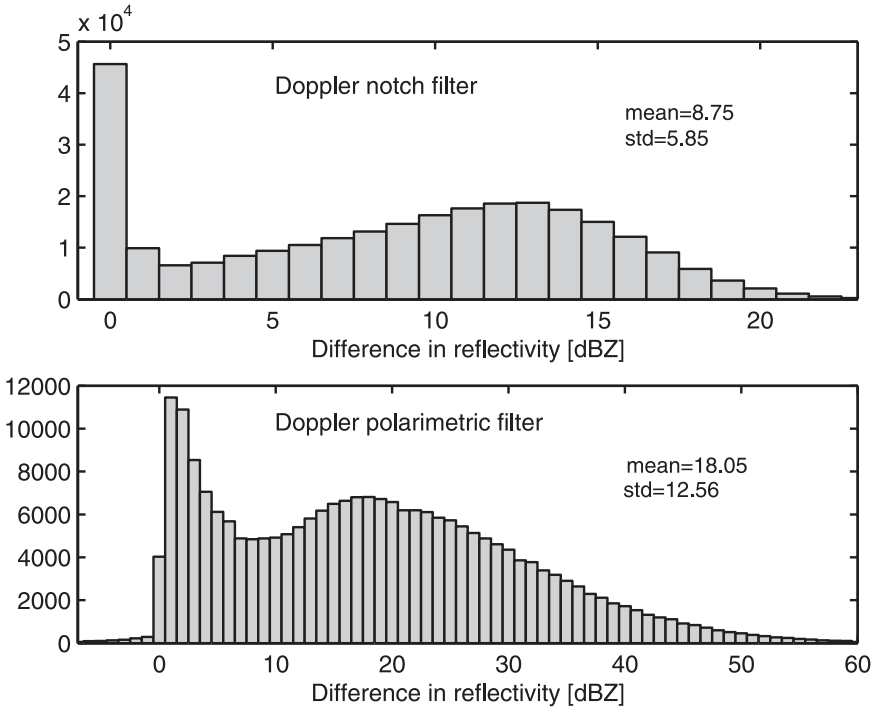

FIG. 15. Histograms of reflectivity differences between the nonfiltered and filtered data (9 Jul 2007) as an illustration of clutter reduction. The Doppler polarimetric filter suppresses clutter-contaminated Doppler bins in the whole Doppler spectrum and not only around 0 m s^{-1}, like the notch filter.

polarimetric filter (bottom panel). For every height, the notch filter suppresses the Doppler bins in the interval [−0.2, 0.2 m s^{-1}]. The raw profiles show a clutter band (−15 to 10 dBZ) for the first 900 m. A weaker-echo clutter band is also visible at the heights of 2000–3000 m. The notch filter substantially removes the clutter bands. However, the Doppler polarimetric filter removes even more clutter. Furthermore, the boundaries of the cloud (13.7–13.8 UTC hours) are recovered, there are much less missing data for the clear-air scattering echo (14.1 and 14.2 UTC hours) and the fine structure of clear-air scattering below 600 m (−25 to −10 dBZ) is nearly entirely recovered. The missing data (top and middle panels) result from the Doppler width mask at the end of the processing. It is again an illustration of loss of data by masking the profiles. Because the Doppler width values are corrected after applying the Doppler polarimetric filter, this mask does not suppress the parameter data (bottom panel). Perhaps the most spectacular is the possibility to retrieve clear-air scattering echoes with their Doppler and polarimetric properties, which have a reflectivity much lower than the clutter (heights 200–900 m).

For this measurement, an illustration of the clutter reduction is given in Fig. 15. Histograms of the differences in reflectivity between the nonfiltered and the filtered data are plotted. The first peak (0 dB and 0–5 dB in the top and bottom panels, respectively) corresponds to the cloud and clear-air echoes readily discernable from clutter. For the bottom panel, the cloud values are mainly between 0 and 1 dB. The boundaries of the cloud and some parts of clear-air echoes show values between 2 and 5 dB. In those areas, both Doppler spectra—atmospheric and clutter—are near the Doppler noise level. Hence, the two consequences of spectral polarimetric filtering on the reflectivity estimates are underestimation and correct reduction. The part of the lower distribution (25–60 dB) is related to the clutter zone, which masks clear-air echoes. The maximum clutter reduction is 23 and 60 dB for the notch and Doppler polarimetric filters, respectively.

c. *Scanning at low elevation angle*

At Cabauw, TARA profiles vertically or slanted. At the same location but on top of a 213-m tall meteorological tower, a new Doppler polarimetric radar designed by the University of Delft has operated at the elevation of 0.5° since 2008. IDRA is an X-band scanning radar (Figueras i Ventura and Russchenberg 2008).

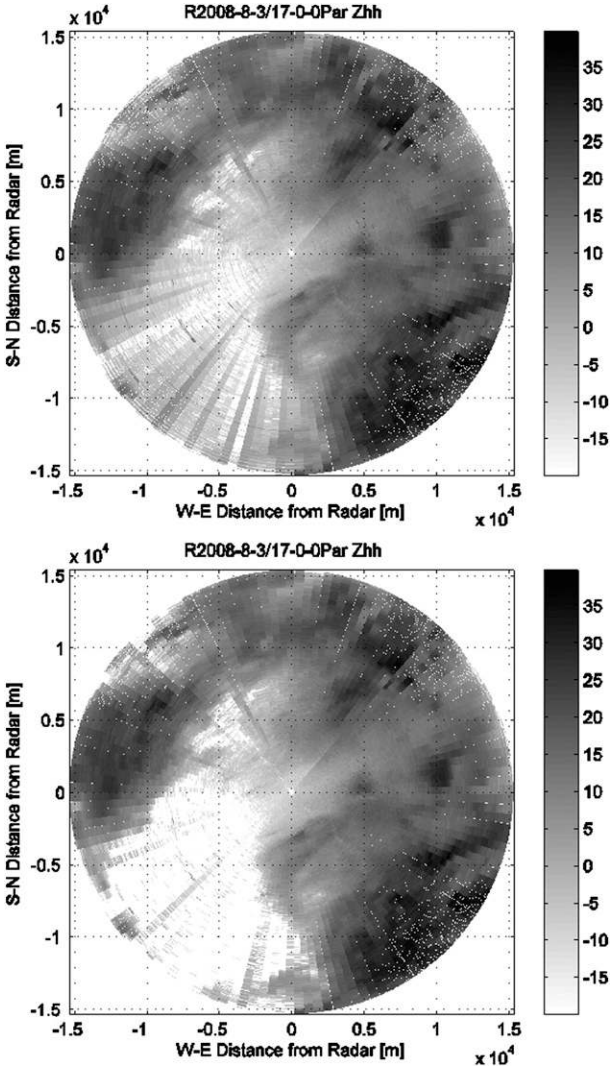

FIG. 16. IDRA reflectivity scans at the elevation of 0.5° (3 Aug 2008) obtained with (top) a notch filter and (bottom) the combination of a notch filter with a double spectral linear depolarization ratio filter.

This highly sensitive radar aims at the observation of the spatial and temporal distribution of rainfall and drizzle. The first clutter suppression is a notch filter of 26 cm s^{-1} around 0 m s^{-1}. Later, after testing, the double spectral linear depolarization ratio filter was added in the real-time processing. The latter filter substantially reduces noise and radial artifacts (see Fig. 16). The cause of these radial artifacts is currently investigated.

8. Conclusions

Radar spectral polarimetry (i.e., radar Doppler polarimetry) is not only important for microphysical and dynamical research on atmospheric targets, but it also provides powerful clutter-suppression techniques. The currently optimum spectral polarimetric clutter-suppression technique, which is based on thresholding, is the double spectral linear depolarization ratio method. This new technique, which is proposed in the paper, uses two Doppler spectra of linear depolarization ratios (sZ_{VH}/sZ_{HH} and sZ_{HV}/sZ_{VV}) and removes the Doppler bins related to values of these parameters larger than −5 dB. Ground clutter and moving clutter such as airplanes, helicopters, and vehicles are suppressed. Because this filter operates on the Doppler spectra, the atmospheric data of the profiles and scans are corrected. For TARA, this operation largely improves the profiles and the spectrographs of rain, precipitating cloud, ice cloud, mixed-phase cloud, and clear-air scattering. Concerning the atmospheric targets, the tails of the melting-layer Doppler spectra are suppressed. A low Doppler signal-to-noise ratio leads to values of the spectral linear depolarization ratios approaching 0 dB and therefore atmospheric targets, such as weak-echo clouds, may be suppressed.

The double spectral linear depolarization ratio filter is successfully tested in a large number of cases and two different sites for 45°–90° elevation with TARA data. Examples of those tests are presented in the paper. Its performances are much better than a classical notch filter. It is expected that this filter operates as well from 0° to 45° elevations and at other frequency bands, such as the C and X bands. This is confirmed by measurements performed with the X-band quasi-horizontally scanning radar IDRA. For our radar, TARA, this new technique of clutter suppression is combined with a robust polarimetric dealiasing technique, which also leads to clutter reduction. We have named this combination the Doppler polarimetric filter.

All the discussed Doppler polarimetric techniques can be easily implemented in real time. They are studied for two averaged and nonaveraged Doppler spectra, where the spectral polarimetric parameters exhibit large statistical variations. The values of the spectral linear depolarization ratios are strongly biased by the signal-to-noise ratio. However, these values, which generally cannot provide microphysical information, can be fruitfully used for clutter suppression.

Acknowledgments. The author acknowledges the support of Climate for Spatial Planning, Earth Research Centre Delft, and the COPS organization committee. Further, the author thanks the Ph.D. students Yann Dufournet and Jordi Figueras i Ventura for their assistance for the COPS TARA data at 45° and the IDRA data, respectively.

APPENDIX A

Polarimetric Dealiasing and Clutter-Suppression Technique

The phase of the cross-correlation coefficient (i.e., differential phase) is determined as the sum of the differential propagation phase and the differential backscattering phase. For an S-band radar, the differential backscattering phase is close to zero. Therefore, the spectral differential phase does not depend on the Doppler velocity and equals the differential propagation phase. For small maximum range (15 km for TARA) and slant or vertical profiles of atmospheric echoes, the differential propagation phase and thus the phase of $s\rho_{co}(v)$ is negligible. In practice and in absence of clutter, the measured spectral phase is related to the actual Doppler velocity of the target when the measurements VV and HH are not simultaneous:

$$s\psi(v) = \frac{4\pi}{\lambda}(v \pm n_D 2v_{D,\max})\Delta t, \qquad \text{(A1)}$$

where Δt is the time difference between the VV and HH measurements, v is the measured Doppler velocity of the target, n_D the number of Doppler aliasing (0, 1), and $v \pm n_D 2v_{D,\max}$ is the actual Doppler velocity of the target. From this property (A1), a dealiasing technique is developed in Unal and Moisseev (2004). The nonsimultaneity of the measurements VV and HH is corrected by multiplying the cross-spectrum phase per Doppler velocity bin (A1) by $-4\pi\ v\ \Delta t/\lambda$. For a sequence of three measurements (VV, HV, and HH), the corrected phase will show three nonambiguous mean values—0 (no aliasing) and $\pm 8\pi\ v_{D,\max}\ \Delta t/\lambda$ ($\pm 120°$)—in presence of Doppler aliasing of the spectrographs. They lead to phase intervals that are related to the three Doppler velocity intervals: $[-3v_{D,\max},\ -v_{D,\max}]$, $[-v_{D,\max},\ v_{D,\max}]$, and $[v_{D,\max},\ 3v_{D,\max}]$. Based on the value of the phase of $s\rho_{co}(v)$, each Doppler bin will be placed in the correct Doppler velocity interval. For the final estimates of spectrographs and moments, the initial interval $[-3v_{D,\max},\ 3v_{D,\max}]$, as a result of the dealiasing, is reduced for clutter and noise suppression to the range-dependent interval $[v(r) - v_{D,\max}, v(r) + v_{D,\max}]$, where $v(r)$ is the mean Doppler velocity.

The phase standard deviation decreases when the number of averages and the modulus of the spectral cross-correlation coefficient increase. Without averaging, phase ambiguity may occur (selecting the wrong Doppler velocity interval) for atmospheric target bins with a spectral cross-correlation coefficient below 0.72 (Unal and Moisseev 2004), or equivalently with a phase standard deviation exceeding 60°.

The combination of noise and different clutter sources has a phase distribution comparable to the uniform distribution before the phase correction. The phase distribution after phase correction shows three wide peaks at $\pm 120°$ and 0°. With this condition, $\frac{2}{3}$ of the noise and approximately $\frac{2}{3}$ of the clutter can be suppressed with the reduction of the Doppler interval after dealiasing.

Contrary to the filter based on the modulus of the spectral cross-correlation coefficient, this method does not require averaging. For noise reduction, the use of $|s\rho_{co}(v)|$ is more effective than the polarimetric dealiasing clutter-suppression technique. This technique may fail when large reflectivity clutter Doppler spectra are placed in a different Doppler velocity interval than low reflectivity atmospheric Doppler spectra. The spectrographs are correctly dealiased but the estimate of the mean Doppler velocity v is wrong. Therefore, the polarimetric dealiasing clutter reduction should be combined with another Doppler polarimetric filter to avoid this possible error.

APPENDIX B

Processing to Obtain the Spectrographs and the Profiles

The processing is carried out on the spectrographs. The Doppler bin 0 m s^{-1} is first removed. Two consecutive Doppler spectra are averaged, there is light smoothing of the resulting Doppler spectrum to reduce the statistical variations, and a classical dealiasing technique (unfolding and continuity check of the spectrographs) is used.

A clipping of 5 dB above the Doppler noise floor is performed (Doppler bins related to spectral reflectivity lower than Doppler noise floor +5 dB are discarded). The value 5 dB results from the trade-off between keeping the entire atmospheric Doppler spectrum as much as possible and optimally removing the noise spectrum in the case of data with statistical variations.

Diverse spectral polarimetric clutter-suppression techniques have been applied on the resulting spectrograph (section 6). They discard Doppler bins related to atypical values of one spectral polarimetric parameter. Instead of the classical dealiasing technique, the polarimetric dealiasing and clutter-suppression method can be applied.

When the resulting spectrograph is obtained, a profile of reflectivity [(3)], mean Doppler velocity [(B1)], and Doppler width [(B2)] is calculated. For the profile of Z_{dr} and L_{dr}, two spectrographs are considered to estimate the reflectivities (Z_{HH}, Z_{VV}) and (Z_{HH}, Z_{VH}), respectively:

$$v_{XY} = \frac{\sum_v v \times sZ_{XY}(v)}{\sum_v sZ_{XY}(v)} \quad \text{and} \tag{B1}$$

$$W_{XY} = \sqrt{\frac{\sum_v (v - v_{XY})^2 \times sZ_{XY}(v)}{\sum_v sZ_{XY}(v)}}. \tag{B2}$$

The current processing for TARA (section 7) is outlined next. After removing the Doppler bin 0 m s^{-1}, two consecutive Doppler spectra are averaged, the polarimetric dealiasing technique is applied on the averaged Doppler spectrum, and the dealiased Doppler spectrum is slightly smoothed. The spectral polarimetric clutter-suppression techniques are combined with the Doppler noise clipping of 5 dB. They consist of applying the new double spectral linear depolarization ratio filter and reducing the dealiased Doppler interval. To reduce the dealiased Doppler interval before the final computation of the moments, a first estimate of the profile of mean Doppler velocity has to be known. For a better estimate, the double $sL_{dr}(v)$ clipping of −5 dB is applied. The spectral differential reflectivity filter and the spectral cross-correlation coefficient filter are not applied.

In the considered cases (diverse spectral polarimetric filters and no filter), the profiles have a time resolution of 3 s. A mask is finally applied on the profiles, which keeps the data related to a Doppler width larger than the Doppler resolution and smaller than 3 m s^{-1}.

REFERENCES

Bachmann, S., and D. Zrnić, 2007: Spectral density of polarimetric variables separating biological scatterers in the VAD display. *J. Atmos. Oceanic Technol.,* **24,** 1186–1198.

Bringi, V. N., and V. Chandrasekar, 2001: *Polarimetric Doppler Weather Radar: Principles and Applications*. Cambridge University Press, 636 pp.

Figueras i Ventura, J., and H. W. J. Russchenberg, 2008: IDRA, a high resolution meteorological radar. *Proc. Fifth European Conf. on Radar in Meteorology and Hydrology*. Helsinki, Finland, Finnish Meteorological Institute, 9.6.

Hagen, M., 1997: Identification of ground clutter by polarimetric radar. Preprints, *28th Int. Conf. on Radar Meteorology,* Austin, TX, Amer. Meteor. Soc., 67–68.

Heijnen, S. H., L. P. Ligthart, and H. W. J. Russchenberg, 2000: First measurements with TARA: An S-band transportable atmospheric radar. *Phys. Chem. Earth,* **25B,** 995–998.

Meischner, P. F., V. N. Bringi, D. Heimann, and H. Holler, 1991: A squall line in southern Germany: Kinematics and precipitation formation as deduced by advanced polarimetric and Doppler radar measurements. *Mon. Wea. Rev.,* **119,** 678–701.

Moisseev, D. N., and V. Chandrasekar, 2007: Nonparametric estimation of raindrop size distributions from dual-polarization radar spectral observations. *J. Atmos. Oceanic Technol.,* **24,** 1008–1018.

——, and ——, 2009: Polarimetric spectral filter for adaptive clutter and noise suppression. *J. Atmos. Oceanic Technol.,* **26,** 215–228.

——, C. Unal, H. Russchenberg, and L. Ligthart, 2000: Doppler polarimetric ground clutter identification and suppression for atmospheric radars based on co-polar correlation. *Preprints, 13th Int. Conf. on Microwaves, Radar and Wireless Communications,* MIKON-2000, Vol. 1, Wroclaw, Poland, 94–97.

Ryzhkov, A., 2001: Interpretation of polarimetric radar covariance matrix for meteorological scatterers: Theoretical analysis. *J. Atmos. Oceanic Technol.,* **18,** 315–328.

——, and D. Zrnić, 1998: Polarimetric rainfall estimation in the presence of anomalous propagation. *J. Atmos. Oceanic Technol.,* **15,** 1320–1330.

Spek, A., C. Unal, D. Moisseev, H. Russchenberg, V. Chandrasekar, and Y. Dufournet, 2008: A new technique to categorize and retrieve the microphysical properties of ice particles above the melting layer using radar dual polarization spectral analysis. *J. Atmos. Oceanic Technol.,* **25,** 482–497.

Unal, C. M. H., and D. N. Moisseev, 2004: Combined Doppler and polarimetric radar measurements: Correction for spectrum aliasing and non simultaneous polarimetric measurements. *J. Atmos. Oceanic Technol.,* **21,** 443–456.

——, ——, and L. P. Ligthart, 1998: Doppler polarimetric radar measurements of precipitation. *Proc. Fourth Int. Workshop on Radar Polarimetry,* Nantes, France, IRESTE, 429–438.

Yanovsky, F. J., H. W. J. Russchenberg, and C. M. H. Unal, 2005: Retrieval of information about turbulence in rain by using Doppler-polarimetric radar. *IEEE Trans. Microwave Theory Tech.,* **53,** 444–450.

Zrnić, D., and A. Ryzhkov, 1999: Polarimetry for weather surveillance radars. *Bull. Amer. Meteor. Soc.,* **80,** 389–406.